Frequency Analysis of PWM Inverters With Dead-Time for Arbitrary Modulating Signals

Fernando Chierchie, *Graduate Student Member, IEEE*, Leandro Stefanazzi, Eduardo E. Paolini, and Alejandro R. Oliva

***Abstract*—The effect of dead-time on the spectrum of pulse-width modulated signals is analyzed in this paper. The study is valid for arbitrary, band-limited modulating signals, extending previous results in the literature. A simple distortion index is developed that can be used at the design stage to select dead-time or switching frequency based on maximum allowed distortion. Experimental results with various band-limited signals reveal a very good agreement between the theoretical results and the experiments.**

***Index Terms*—Dead-time distortion, digital modulation, frequency spectrum, harmonic distortion, power amplifier, pulse-width modulation (PWM), switching amplifier.**

NOMENCLATURE

$x_m(t)$	Modulating signal.
$v_o(t)$, $v_{o,id}(t)$	Actual and ideal (no dead-time) PWM output voltage (load voltage).
$e(t)$	Error signal: $v_{o,id}(t) - v_o(t)$.
$i_o(t)$	Output current (load current).
$i_{o,\mathrm{LF}}(t)$, $i_{o,\mathrm{HF}}(t)$	Frequency decomposition of $i_o(t)$.
$Z_L(s) = Y(s)^{-1}$	Load impedance.
$p_s(t)$, $p_c(t)$	Component of $v_o(t)$ and $v_{o,id}(t)$ dependent and nondependent on $x_m(t)$.
$p_\Delta(t)$	Pulse of unit amplitude and duration Δ.
$P_c(f), P_s(f), E(f)$	Fourier transforms of $p_c(t)$, $p_s(t)$, and $e(t)$.
$P_{c,p}(f), P_{s,p}(f), E_p(f)$	Fourier transforms of one period of $p_c(t)$, $p_s(t)$, and $e(t)$.
$P_\Delta(f), V_o(f), I_o(f)$	Fourier transforms of $p_\Delta(t)$, $v_o(t)$, and $i_o(t)$.
C_k, C_k^e, C_k^x	Complex Fourier series coefficients of $v_o(t)$, $e(t)$, and $x_m(t)$.
Δ	Dead-time (seconds).
T, $f_c = 1/T$	PWM period and frequency.
T_m, $f_m = 1/T_m$	Period and frequency of $x_m(t)$, when it is periodic.
$\sigma(t)$	Choice function: $\sigma(t) = [1 + \mathrm{sgn}(i_o(t))]/2$.
t_k	Falling edge location (seconds) of the kth interval
τ_k	Pulse width for the kth interval.
$\varphi, \lambda = \varphi T_m/(2\pi)$	Angle and time delay between the fundamental components of $v_o(t)$ and $i_o(t)$.
k_1, k_2	PWM period indexes, where $i_o(t)$ changes its sign.
λ_1, λ_2	Time between the beginning of the $k_i T$ PWM period and sign transition of $i_o(t)$.
τ_{k_1}, τ_{k_2}	Pulse widths correspondent to k_1 and k_2 interval.
ρ_1, ρ_2	Indicates if $v_o(t)$ is at $V(+)$ or $V(-)$, when $i_o(t)$ changes its sign.
D	Distortion level introduced by dead-time.
THD [dB]	Total harmonic distortion in decibels.

Manuscript received March 7, 2013; revised May 10, 2013; July 15, 2013; accepted July 19, 2013. Date of current version January 29, 2014. This work was supported in part by CONICET, CIC and SGCyT-UNS (PGI 24ZK21 and PGI 24K055) PAE-PICT-2007-02344. Recommended for publication by Associate Editor C. N. M. Ho.

F. Chierchie and A. R. Oliva are with the CONICET, Instituto de Investigaciones en Ing. Electrica (IIIE) Alfredo Desages (UNS-CONICET) and the Dto. de Ing. Electrica y de Computadoras, Universidad Nacional del Sur, 8000 Bahia Blanca, Argentina (e-mail: fernando.chierchie@uns.edu.ar; aoliva@uns.edu.ar).

L. Stefanazzi is with the INTI, Instituto de Investigaciones en Ing. Electrica (IIIE) Alfredo Desages (UNS-CONICET) and the Dto. de Ing. Electrica y de Computadoras, Universidad Nacional del Sur, 8000 Bahia Blanca, Argentina (e-mail: lstefanazzi@uns.edu.ar).

E. E. Paolini is with the CIC, Instituto de Investigaciones en Ing. Electrica (IIIE) Alfredo Desages (UNS-CONICET) and the Dto. de Ing. Electrica y de Computadoras, Universidad Nacional del Sur, 8000 Bahia Blanca, Argentina (e-mail: epaolini@uns.edu.ar).

Color versions of one or more of the figures in this paper are available online at http://ieeexplore.ieee.org.

Digital Object Identifier 10.1109/TPEL.2013.2276098

I. INTRODUCTION

THE finite turn-off and turn-on times of the switches of a voltage source inverter require delaying the turn-on control signal by adding a dead-time (also known as blanking time) to avoid a short circuit between the dc source and ground, a drawback known as "shoot through" or cross conduction. As a consequence, the quality of the output waveform is degraded, reducing the RMS value of the fundamental output voltage and increasing the baseband distortion, an effect that cannot be eliminated by low-pass filtering. Previous studies include the analysis of its effects for resonant converters [1], the detection of optimal dead-times for dc–dc converters [2], and a behavioral model of a voltage source inverter with dead-time [3].

An analytical model of the spectrum of pulse-width modulation (PWM) signals with dead-time has been first developed in [4] for sinusoidal inputs and later extended to multilevel PWM in [5]. An approach including other circuital effects is presented in [6] and the analysis is extended to the frequency domain in [7]. These developments are based on the double Fourier series approach introduced by Black in 1953 [8],

0885-8993 © 2013 IEEE. Personal use is permitted, but republication/redistribution requires IEEE permission.
See http://www.ieee.org/publications_standards/publications/rights/index.html for more information.

and therefore, the results are only valid when the modulating signal is a single-frequency sinusoid. Another recent approach has been developed for a single-frequency signal, and, according to the authors, it can be easily extended for multiple-frequency reference signals with relatively minor modifications but a considerable amount of additional algebra [9]. Extending these results for arbitrary signals is not straightforward due to the nonlinear nature of PWM and dead-time effects on the output voltage.

The frequency spectrum of ideal PWM signals for arbitrary, band-limited inputs has been developed recently [10]. This paper uses this approach to derive the spectrum of PWM signals with dead-time for finite bandwidth signals. The analysis is exhaustive, including the typical assumption that the output current changes its sign only twice per cycle (TEC mode) [4], [9], [11] as a particular case.

Choosing the maximum switching frequency and the amount of dead-time is critical for the performance of switched systems, and hence, knowing its effects in advance is of paramount importance. Based on the expressions of the spectrum of the error signal produced by dead-time, a distortion index for arbitrary modulating signals is derived. This index is easy to compute, and depends only on the dead-time value and the PWM period. It is shown that it provides a very good estimation of the THD value, and it is simpler to compute than other approaches [12].

These results can be used for the analysis of dead-time effects in a variety of problems such as arbitrary waveform generation [13], class-D amplification [14], [15], series active power filters [16], etc., where it may be necessary to predict the voltage distortion when finite bandwidth signals are used for the modulation. For other applications such as grid-connected PWM inverters [17], parallel active filtering [18], and motor drives [19], the controlled output variable is current; in these cases, the shape of the current not only depends on the inverter, but it is also affected by the nonlinearities of the attached load, including nonsinusoidal voltage sources that may model distortion of the utility voltage or the back EMF of the motor. The distortion of the output current of such inverters is out of the scope of this paper, which only focuses on the output voltage.

The main contributions of this paper are: 1) the extension of previous results for determining the frequency spectrum of the PWM signals with dead-time for arbitrary signals with finite bandwidth, in particular, the effect of dead-time on the PWM spectrum for arbitrary, periodic, modulating signals; 2) the development of a design tool based on easily computable distortion index that helps to choose the carrier frequency or the dead-time according to a certain distortion level; 3) the comparison of theoretical results with the experimental measurements of the frequency spectra of PWM waveforms with dead-time using an H-bridge and a digital signal processor (DSP) for various band-limited signals.

The organization of this paper is as follows. In Section II, the effect of dead-time on the output voltage is analyzed in the time domain. The spectrum of the PWM signals with dead-time for arbitrary modulating signals is developed in Section III with stronger results in the case of periodic modulating signals. The analytical and experimental results are compared in Section IV, and some conclusions are discussed in Section V.

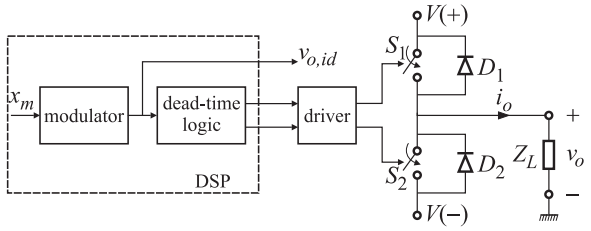

Fig. 1. Inverter leg.

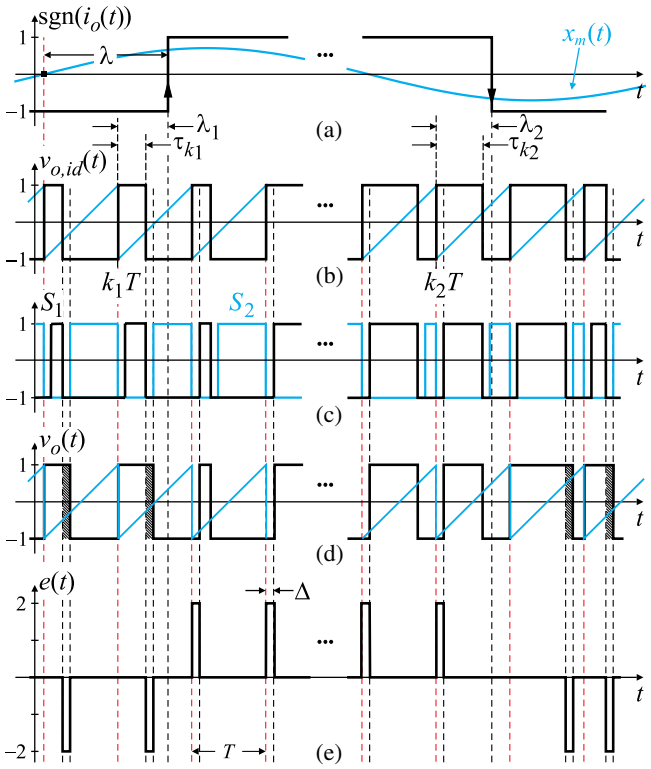

Fig. 2. Time-domain effect of dead-time: (a) $x_m\,(t)$ and sign of $i_0\,(t)$; (b) ideal PWM $v_{o,id}\,(t)$ and sawtooth carrier; (c) gate signals for the switches S_1 and S_2; (d) actual PWM $v_o\,(t)$ and sawtooth carrier; (e) error $e(t) = v_{o,id}\,(t) - v_o\,(t)$.

II. Effect of Dead-Time on the Output Voltage

Dead-time (or blanking time) is a delay Δ introduced in the switching of the control signals driving the gates of the power transistors of an inverter to avoid shoot through. Fig. 1 shows a typical inverter leg (or inverter arm) composed of switches S_1, S_2; diodes D_1, D_2; power supplies $V(+)$, $V(-)$; and the load Z_L; v_o is the output voltage and i_o is the load current.

The delay Δ is added to the rising edge of the signals that drives both switches. This can be noticed by comparing the ideal PWM signal $v_{o,id}(t)$ in Fig. 2(b) with the actual driving signals in Fig. 2(c). As shown in [20], since both switches are `off` during the blanking time, v_o depends on the direction of i_o in this interval. When the ideal PWM signal changes from `low` to `high`, the transition of the signal that drives the switch S_1 is delayed by the blanking time Δ. If $i_o > 0$ in this interval, then i_o flows by D_2 and v_o is clamped to $V(-)$ instead of switching to $V(+)$. The net effect is a widening of the previous PWM `off` pulse, causing a loss of area and lowering the average output

voltage; the effect is more pronounced when the modulation index is small [20]. On the other hand, when $i_o < 0$, the current flows through D_1 clamping v_o at $V(+)$; in this situation, the output changes to the desired state at the proper instant, and the blanking time Δ has no effect on the behavior of the ideal PWM signal. A similar analysis can be carried out for the `high` to `low` transition, but in this case, a widening of the `on` pulse occurs if $i_o < 0$, and no effect is observed if $i_o > 0$.

The difference between the ideal PWM output $v_{o,id}(t)$ and the actual one $v_o(t)$ is the error signal due to dead-time

$$e(t) = v_{o,id}(t) - v_o(t).$$

This signal is composed of trains of positive and negative pulses of amplitude $V(+) - V(-)$; the positive (negative) pulses shorten (widen) the PWM pulse, as shown in Fig. 2. The sign of the current flowing through the load is represented in Fig. 2(a), and the ideal PWM signal in Fig. 2(b). The gate signals for the switches S_1 and S_2 are shown in Fig. 2(c). The actual output PWM signal (with dead-time) is depicted in Fig. 2(d), and the error signal $e(t)$ is shown in Fig. 2(e). The PWM carrier is also represented in Fig. 2(b) and (d).

III. Spectrum of the PWM Signal With Dead-Time

To simplify the presentation, in the following PWM trailing edge modulation [21] will be considered: the positive edge of the ideal PWM signal is fixed at kT, where T is the PWM switching period, and the position of the negative edge occurs at $t_k = kT + \tau_k$, where τ_k is the pulse width for the kth interval, and depends on the modulation. Without loss of generality, it will be assumed that $V(+) = -V(-) = 1$.

The PWM signal with zero dead-time can be decomposed into two parts [10]: a symmetrical square wave $p_c(t)$ with an amplitude of ± 1 and a fixed duty cycle of 50%, and a bipolar pulse train $p_s(t)$ which depends on the modulating signal $x_m(t)$, i.e.,

$$v_{o,id}(t) = p_c(t) + p_s(t). \tag{1}$$

The rising edge of $p_c(t)$ occurs at $t = kT$, and the falling edge at $t = (k + 1/2)T$, and therefore, it is a zero mean, periodic square wave with the same frequency of the PWM carrier

$$p_c(t) = \sum_{k=-\infty}^{\infty} u(t - kT) - u\left[t - \left(k + \frac{1}{2}\right)T\right].$$

Its Fourier transform is

$$P_c(f) = \sum_{k=-\infty}^{\infty} \frac{-2j}{2k+1}\delta\left(f - \frac{2k+1}{T}\right) \tag{2}$$

where $\delta(\cdot)$ is the Dirac delta function.

The bipolar pulse train $p_s(t)$ has a fixed edge at $(k + 1/2)T$, but the position of the other edge depends on the modulating signal $x_m(t)$ through τ_k, where $0 < \tau_k < T$. Within any interval $[kT,\ (k+1)T]$, $p_s(t)$ is described by a pulse of amplitude 2, negative if $\tau_k < T/2$ and positive if $\tau_k > T/2$

$$p_s(t) = 2\sum_{k=-\infty}^{\infty} u\left[t - \left(k + \frac{1}{2}\right)T\right] - u\left[t - (kT + \tau_k)\right]$$

where $u(t)$ is the unit step function. The spectrum of $p_s(t)$ is

$$P_s(f) = \frac{-j}{\pi f}\sum_{k=-\infty}^{\infty} e^{-j2\pi f(k+\frac{1}{2})T} - e^{-j2\pi f(kT+\tau_k)}. \tag{3}$$

The actual PWM signal with dead-time can be expressed as

$$\begin{aligned} v_o(t) &= v_{o,id}(t) - e(t) \\ &= p_c(t) + p_s(t) - e(t) \end{aligned} \tag{4}$$

where the error signal $e(t)$ is a bipolar pulse train of amplitude 2, with positive pulses when $i_o > 0$ and negative pulses when $i_o < 0$, as shown in Fig. 2(e). The width Δ of the pulses is fixed, and equals the duration of the dead-time. Therefore, the error signal $e(t)$ can be expressed as the time convolution of a pulse

$$p_\Delta(t) = 2[u(t) - u(t - \Delta)] \tag{5}$$

whose Fourier transform is

$$P_\Delta(f) = 2\Delta\text{sinc}(\Delta f)e^{-j\pi\Delta f} \tag{6}$$

with an impulse train formed by Dirac-delta impulses $\delta(t - kT)$ or $-\delta(t - t_k)$, one in each period of the PWM signal. The sign of the impulses and their location depends on the sign of the output current $i_o(t)$. Positive impulses occur when $i_o > 0$ and are located at $t = kT$. Negative impulses appear at $t = t_k$ when $i_o < 0$, where t_k depends on the modulating signal $x_m(t)$. The spectrum of $e(t)$ can be written as [22]

$$E(f) = \sum_{k=-\infty}^{\infty} e^{-j2\pi t_k f} P_\Delta(f)[\sigma(kT)e^{j2\pi\tau_k f} + \sigma(t_k) - 1] \tag{7}$$

where $\sigma(t)$ is the choice function

$$\sigma(t) = \begin{cases} 1, & \text{if } i_0(t) > 0 \\ 0, & \text{otherwise.} \end{cases}$$

According to (4), the spectrum of the PWM signal with dead-time is given by

$$V_o(f) = P_c(f) + P_s(f) - E(f) \tag{8}$$

showing that dead-time adds new frequency content $E(f)$ given by (7), that was absent in the ideal PWM signal, and that depends on both the dead-time value Δ and the sign of the output current $i_o(t)$ that is reflected by the choice functions $\sigma(kT)$ and $\sigma(t_k)$ in (7). The spectral characteristic of $E(f)$ for two different scenarios is addressed next.

A. Generic Band-Limited Modulating Signals

The complete spectrum of the PWM signal with dead-time when the modulating signal is any arbitrary band-limited signal is given by (8), where the effect of dead-time is represented by $E(f)$ that can be computed with (7). Without further assumptions on the modulating signals, it is not possible to find more compact expressions for the PWM spectrum.

B. Periodic Band-Limited Modulating Signals

The effect of dead-time on the spectrum of PWM signals can be further refined when the band-limited modulating signals

$x_m(t)$ are periodic. Hereinafter, it will be assumed that $x_m(t)$ and $i_o(t)$ are T_m-periodic, where the signal period $T_m = 1/f_m$ and the carrier period T are in integer relation, $T_m = mT$[1]. Under these hypotheses, $e(t)$ is periodic and a Fourier series analysis is feasible: the periodic PWM signal $v_o(t)$ can be expressed as

$$v_o(t) = \sum_{k=-\infty}^{\infty} C_k e^{j\frac{2\pi}{T_m}k\,t}. \tag{9}$$

The coefficients C_k are obtained by sampling one period of its Fourier Transform [22]

$$C_k = \frac{1}{T_m}\left[P_{c,p}(f) + P_{s,p}(f) - E_p(f)\right]\Big|_{f=\frac{k}{T_m}} \tag{10}$$

where $P_{c,p}(f)$, $P_{s,p}(f)$, and $E_p(f)$ are the Fourier transforms of one period of $p_c(t)$, $p_s(t)$, and $e(t)$, respectively.

The error signal $e(t)$ is also periodic, and its period is composed of m total pulses like (5), the positives located at $t = kT$ and the negatives at $t = kT + \tau_k$. The Fourier coefficients of $e(t)$ can be computed as

$$C_k^e = \frac{1}{T_m}E_p(f)\Big|_{f=\frac{k}{T_m}}. \tag{11}$$

Because $e(t)$ is now periodic, $E_p(f)$ can be computed summing (7) over one period

$$E_p(f) = P_\Delta(f)\sum_{k=0}^{m-1} e^{-j2\pi t_k f}\left[\sigma(kT)e^{j2\pi\tau_k f} + \sigma(t_k) - 1\right]. \tag{12}$$

A closed-form expression for the spectrum of PWM signals with dead-time requires the derivation of an explicit relationship between the occurrence of the PWM pulses and the sign of the output current $i_o(t)$ to remove the dependence of (12) on the choice functions $\sigma(t)$.

If the load impedance is linear, and its Laplace transform $Z_L(s)$ is known, the steady-state output current $i_o(t)$ can be computed from $v_o(t)$ as follows. The Fourier transform of $i_o(t)$ can be written as $I_o(f) = Z_L^{-1}(f)V_o(f)$, and according to (9)

$$i_o(t) = \sum_{k=-\infty}^{\infty} Y_k C_k e^{j\frac{2\pi}{T_m}k\,t} \tag{13}$$

where $Y_k = |Y_k|e^{j\arg(Y_k)} = Z_L^{-1}(j2\pi k/T_m)$ is the complex value of the admittance $Z_L^{-1}(s)$ at $s = j2\pi(kf_m) = j2\pi(k/T_m)$. To simplify the analysis, the output current is approximated by a low-frequency component $i_{o,\mathrm{LF}}(t)$, that results of the application of voltage $x_m(t)$ on admittance $Y(s)$, and a high-frequency component $i_{o,\mathrm{HF}}(t)$, with a fundamental frequency equal to the carrier frequency $f_c = 1/T$, i.e.,

$$i_o(t) = i_{o,\mathrm{LF}}(t) + i_{o,\mathrm{HF}}(t) \tag{14}$$

[1]This analysis can be easily adapted for the case of discrete-time modulators that derive the signal and carrier frequencies from a single master clock of frequency $1/T_c$ by choosing $T_m/m_1 = T/m_2 = T_c$ for $m_1, m_2 \in \mathbb{Z}$.

with

$$i_{o,\mathrm{LF}}(t) \approx \sum_k |Y_k| C_k^x e^{jk\frac{2\pi}{T_m}t + \arg(Y_k)} \tag{15}$$

where C_k^x are the Fourier series coefficients of $x_m(t)$. The high-frequency (ripple) component $i_{o,\mathrm{HF}}(t)$ can be approximated with a few terms of the Fourier series of the square wave $p_c(t)$ filtered by the admittance $Y(s)$

$$i_{o,\mathrm{HF}}(t) \approx \sum_{k=1,3,5} \frac{4}{\pi k}|Y_k|\sin[2\pi f_c k t + \arg(Y_k)]. \tag{16}$$

Therefore, $i_o(t)$ can be computed with (14), where the low-frequency component of the current (15) is due to $x_m(t)$ and the high-frequency (ripple) component $i_{o,\mathrm{HF}}(t)$ (16) is due to the harmonics of $p_c(t)$.

This approximation provides enough information for the computation of $\sigma(t)$ because it depends only on the zero crossings of the current and not on its exact form. Under this setting, the Fourier components of the error signal can be computed using (11) with $\sigma(t) = [1 + \mathrm{sgn}(i_o(t))]/2$ using (14) for $i_o(t)$, and hence, only Δ and $Z_L(s)$ are required to compute the spectrum. This approach is appropriate for a wide range of output current values. In certain applications, one of the terms in (14) may dominate over the other. For example, in class-D amplifiers, $i_{o,\mathrm{HF}}(t)$ may dominate when $v_o(t)$ is small (i.e., during very soft passages of the musical score), while in power converters driving a heavy load usually the low-frequency components $i_{o,\mathrm{LF}}(t)$ (15) dominates.

In this latter case, if it is assumed that $i_o(t)$ changes sign only twice per cycle of the modulating signal, the analysis can be further simplified by approximating its behavior with the "two even crossover" (TEC) mode [4]. In this case, computation of $\sigma(t)$ only requires the knowledge of the load power factor $\cos\varphi$ that introduces a delay λ between the fundamental Fourier component of voltage and current waveforms, i.e., $\lambda = (\varphi T_m)/(2\pi)$. The sign of the current i_o changes within the intervals k_1 and k_2 given by $k_1 = \lfloor \lambda/T \rfloor$ and $k_2 = \lfloor \lambda/T + T_m/(2T) \rfloor$, where $\lfloor x \rfloor$ stands for the floor function (the greatest integer less than x). The time interval between the sign transition and the beginning of the interval ($k_i T$ for $i = 1, 2$) is $\lambda_1 = \lambda - k_1 T$, $\lambda_2 = \lambda + T_m/2 - k_2 T$ (see Fig. 2). The change of direction of the current when the PWM output is `high` or `low` is indicated by means of the choice functions ρ_1 and ρ_2 given by

$$\rho_i = \begin{cases} 1, & \text{if } \lambda_i - \tau_{k_i} > 0 \\ 0, & \text{otherwise.} \end{cases}$$

Defining $k_3 = k_1 + T_m/T + \rho_1 - 1$, the Fourier transform of one period of the error signal can be expressed as

$$E_p(f) = E_{1,p}(f) + E_{2,p}(f) \tag{17}$$

where

$$E_{1,p}(f) = P_\Delta(f)\sum_{k=k_1+1}^{k_2} e^{-j2\pi f(kT)}$$

$$= e^{-j(k_1+k_2+1)\pi T f} P_\Delta(f)\frac{\sin[(k_2-k_1)\pi T f]}{\sin(\pi f T)} \tag{18}$$

and

$$E_{2,p}(f) = -P_\Delta(f) \sum_{k=k_2+\rho_2}^{k_3} e^{-j2\pi f(kT+\tau_k)}. \quad (19)$$

The module of $E_{1,p}(f)$ has the shape of a Dirichlet kernel weighted by a sinc [the module of the spectrum of $P_\Delta(f)$, see (6)], and its maximum value is $(k_2 - k_1)\Delta \approx \Delta T_m/(2T) = m\Delta/2$. The module of $E_{2,p}(f)$ is similar to that of $E_{1,p}(f)$ when the modulating index is small ($\tau_k \approx T/2$), because negative pulses are almost equally spaced, located approximately at $(k + 1/2)T$. Extensive simulation results show that the magnitude of odd and even Fourier coefficients of $|E_{2,p}(f)|_{f=k/T_m}$ can be both bounded by the magnitude of odd Fourier coefficients of $|E_{1,p}(f)|_{f=k/T_m}$. In other words, the spectrum of the error signal may be considered to be somewhat independent of the modulating signal in the TEC operation mode.

The Fourier coefficients (11) of the error signal, where $E_p(f)$ is computed with (17)–(19), provide a precise characterization of the distortion caused by dead-time in PWM inverters. The distortion depends on the load power factor $\cos\varphi$, the modulating signal $x_m(t)$, and the dead-time Δ:

1) The power factor affects the distribution and quantity of positive and negative error pulses. If $T_m/T = m$ is even, the difference between positive and negative pulses may be 1, 0, or -1; but if T_m/T is odd such difference may range from -2 to 2, depending on the power factor $\cos\varphi$. In either case, the dead-time causes a reduction of the RMS voltage (inductive load) because of the loss of net pulse area, one of the known undesired phenomena caused by dead-time [23].
2) The dead-time duration directly affects the magnitude of the error signal, as shown by (6) and (12).

C. Bound on the Distortion Level

In many applications, it is useful to estimate the distortion level caused by a given Δ/T ratio. A bound is provided by the magnitude of the Fourier coefficients of $E_p(f)$ in (12)

$$|C_\ell^e| = \frac{1}{T_m}\left|E_p\left(\frac{\ell}{T_m}\right)\right| \le \frac{\left|P_\Delta\left(\frac{\ell}{T_m}\right)\right|}{T_m} \sum_{k=0}^{m-1}\left|\sigma(kT)e^{j2\pi\tau_k\frac{\ell}{T_m}} + \sigma(t_k) - 1\right| \quad (20)$$

Taking into account (6), the bound (20) can be written as

$$|C_\ell^e| \le \frac{2\Delta}{T_m}\left|\mathrm{sinc}\left(\frac{\Delta}{T_m}\ell\right)\right| m \le \frac{2\Delta}{T}\left|\mathrm{sinc}\left(\frac{\Delta}{T}\frac{\ell}{m}\right)\right| \quad (21)$$

and considering that $\Delta \ll T$, and that m is usually large, the Fourier coefficients of the error signal due to dead-time can be bounded by

$$|C_\ell^e| \le \frac{2\Delta}{T} \quad (22)$$

at least for $\ell \ll m$, i.e., for all the harmonic comprised within the baseband. Since (21) does not depend on the position of the error pulses, the bound in (22) is independent of the waveform of the carrier (sawtooth or triangular).

Previous results [4] have shown that the magnitude of the harmonics produced by the dead-time is proportional to the dead-time value Δ; (22) not only provides a qualitative bound, but it is also applicable to arbitrary, bandlimited, periodic modulating signals, bounding the maximum amplitude of the Fourier coefficients of the periodic error signal. It can be used as a measure of distortion caused by dead-time. Therefore, we define the *distortion level* D (in dB) due to dead-time as

$$D = 20\log\left(\frac{2\Delta}{T}\right) \quad (23)$$

that is suitable for arbitrary, bandlimited, periodic modulating signals.

Distortion level D depends only on the ratio Δ/T between the dead-time Δ and the carrier period T. In other words, D cannot be reduced by solely increasing the carrier frequency, but power semiconductors with faster switching times relative to the carrier frequency are required.

The distortion level D can be easily related to the THD index. According to Parseval relation [22], the total harmonic distortion is given by

$$\mathrm{THD} = \frac{1}{T_m}\int_{T_m} |e_p(t)|^2 dt = \sum_\ell |C_\ell^e|^2. \quad (24)$$

This expression gives the THD for the entire frequency band. However, in applications, interest is restricted to the baseband, and therefore, only a finite number of harmonics intervenes in the computation of (24). If the baseband comprises only k_b harmonics, the THD within the baseband can be expressed as

$$\mathrm{THD} = \sum_{\ell=-k_b}^{k_b} |C_\ell^e|^2 \quad (25)$$

and according to (22)

$$\mathrm{THD} \le (2k_b + 1)\left(2\Delta/T\right)^2.$$

Therefore, a relationship between D and the THD expressed in dB can be found

$$\mathrm{THD\ [dB]} \le D + 10\log(2k_b + 1) \approx D + 3 + 10\log(k_b).$$

In many cases, this can be a very conservative result, because it does not take into account that usually the amplitude of the harmonics of the error signal decrease with increasing frequency, at least in the baseband. Assuming that the dB value of the harmonics of the error signal C_ℓ^e are bounded from above with a line of slope $\alpha < 0$ starting from a maximum value D, i.e., $|C_\ell^e| \le 10^{D(1-|k|\alpha)/20}$, a closer bound on the THD can be obtained by replacing this expression in (24)

$$\mathrm{THD\ [dB]} \le 20\log\left(\frac{2\Delta}{T}\right) + 20\log\sqrt{\frac{(2\Delta/T)^{2\alpha}+1}{(2\Delta/T)^{2\alpha}-1}} \le D + 10\log\left[\frac{(2\Delta/T)^{2\alpha}+1}{(2\Delta/T)^{2\alpha}-1}\right]. \quad (26)$$

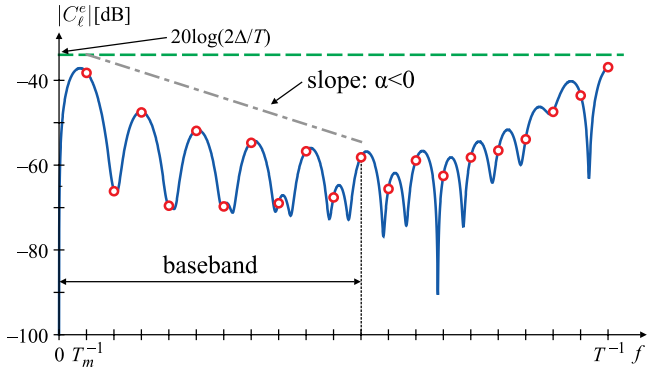

Fig. 3. Spectrum of one period of $e(t)/T_m$ (—); Fourier coefficients $|C_\ell^e|$ of $e(t)$ (○); error bound $20\log(2\Delta/T)$ (– –); line with slope $\alpha < 0$ (– · –). In all cases, $T_m/T = m = 20$, $\Delta/T = 0.01$.

The bound on the THD computed with (26) only requires knowledge of the switching period T, the dead-time value Δ, and the harmonic attenuation rate α. For typical values of these parameters, $(2\Delta/T)^{2\alpha} \gg 1$, and hence, the second term in (26) is small. Therefore, the THD expressed in dB can be approximated with the distortion level D, i.e.,

$$\text{THD [dB]} \approx D \tag{27}$$

requiring an extremely simple computation.

Fig. 3 shows the scaled version of the spectrum $|E_p(f)/T_m|$ and the Fourier coefficients $|C_\ell^e|$ of one period of the error signal $e(t)$ for $\Delta/T = 0.01$ and $T_m/T = 20$. The distortion level ($D \approx -33.9794$) and the line: $D(1 - |k|\alpha)$ that bounds the baseband harmonics are also depicted. The actual THD computed with (25) gives THD [dB] $= -34.1627$, the bound on the THD computed with (26) turns out to be very tight giving -33.9759 dB using $\alpha = -1$ and -33.9793 dB for $\alpha = -2$. This example confirms that in many practical cases, the distortion level D provided by (23) is a useful approximate estimation for the THD.

IV. Examples

Based on the analysis of previous sections, the spectrum of PWM signals with dead-time was computed and measured for several modulating signals. The duty cycles τ_k can be directly computed as a proportional value of the modulating signal samples: $\tau_k = T[x_m(kT) + 1]/2$ (for $-1 < x_m(t) < 1$, known as uniform PWM) or any other digital PWM alternative with better spectral properties can be used. In this paper, the duty cycles τ_k are computed using a digital algorithm (click modulation, see [24]), that allows to specify a frequency band of interest that remains free from modulation distortion components. Therefore, in-band distortion depends entirely on the dead-time effects allowing a better analysis of the spectral measurements. Other modulation schemes such as uniform PWM will affect the frequency content of the baseband through $P_s(f)$ in (3).

A. Experimental Setup

A prototype H-bridge switching amplifier, shown in Fig. 4, was built using standard components (driver MCP14700 and switches IRF8313). The PWM signals and the dead-times are generated with a TMS320F28335 digital signal processor. The duty cycles are computed offline and stored in the DSP's memory. Other parameters are $V(+) = -V(-) = 12$ V, $Z_L(s) = sL + R$ with $L = 166$ μH, $R = 5$ Ω.

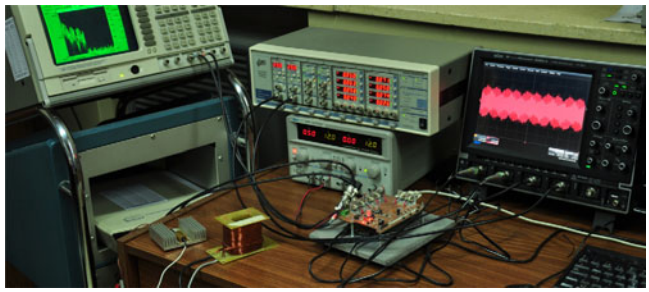

Fig. 4. Experimental setup.

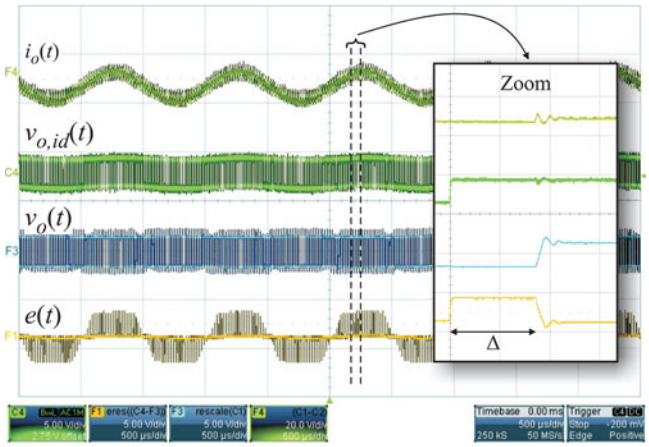

Fig. 5. Experimental reproduction of Fig. 2 with detailed view of an actual error pulse.

B. Experiences

The signals in Fig. 2 were reproduced experimentally to confirm the theoretical model for dead-time, as depicted in Fig. 5 that shows a capture of the oscilloscope's screen. The output current $i_o(t)$ (top trace F4) is measured as the voltage difference across the load resistor. The ideal PWM signal $v_{o,id}(t)$ (trace C4), with no dead-time, is measured at a DSP output pin (see Fig. 1). The actual PWM signal $v_o(t)$ (trace F3) is rescaled to account for the gain of the amplifier. Finally, the error signal $e(t)$ (bottom trace F1) is computed as the difference of both PWM signals (F1 = C4 − F3). The error pulses agree with the theoretical description of Section II. A detailed view of the waveforms is also depicted in Fig. 5, where an actual positive error pulse of duration Δ can be observed. The transition between positive and negative error pulses in trace F1 is not seen as abrupt as in Fig. 2 due to the effect of the high-frequency component of the current $i_{o,\mathrm{HF}}(t)$ during the change of polarity of $i_o(t)$. At this low-amplitude current level, diodes D_1 and D_2 may not be fully turned ON for some switching periods, and hence, some of the error pulses have lower amplitude during the transition. Although the theoretical analysis does not include this phenomenon, the experimental results described below show

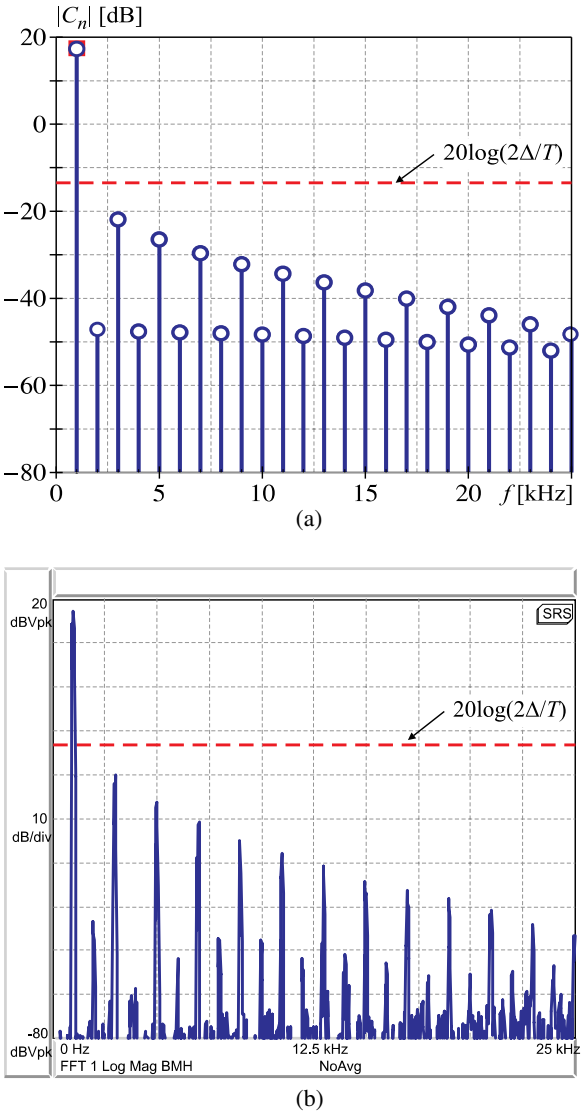

Fig. 6. PWM spectra with dead-time for a sinusoidal modulating signal with $f_m = 1$ kHz, $f_c = 200$ kHz ($m = 200$). (a) Theoretical results and (b) measurements. (a) $\Delta = 0$ (□); $\Delta/T\ [\%] = 1\%$ (50 ns) (○). (b) $\Delta/T\ [\%] = 1\%$ (50 ns).

that the proposed model is still very accurate to capture the effect of dead-times on the output voltage spectrum.

1) Single-Frequency Sinusoid: A sinusoid of frequency $f_m = 1/T_m = 1$ kHz is modulated using a carrier frequency of $f_c = 1/T = 200$ kHz ($m = 200$). The dead-time was set at $\Delta/T\ [\%] = 1\%$ (50 ns). Since m is high, the amplitude of the high-frequency component of the current $i_{o,\mathrm{HF}}(t)$ is low because of the low-pass filtering action of Z_L, and hence, this example can be framed in the TEC operating mode described in Section III-B. Therefore, the Fourier coefficients of the output voltage $v_o(t)$ were computed with (10) and using (18)–(19) for $E_p(f)$, and their amplitude are depicted in Fig. 6(a). The spectrum for $\Delta = 0$ is also shown (a single harmonic at $f = 1$ kHz, noted by a red square), revealing the importance of dead-time in the output signal distortion. Even for this simple case, when the modulating signal is a single-frequency sinusoid, (10) and (18)–(19) do not provide a closed-form expression of the harmonic coefficients, such as those given in [9]. However, this is not really a serious drawback in this case, when f_c and f_m are in integer relationship ($f_c/f_m = m$), because these expressions provide the exact contribution for any harmonic k. (The approach in [9] requires to sum all the overlapping harmonics α of the modulator and β of the carrier, $\alpha, \beta \in \mathbb{Z}$, such that $\alpha + \beta m = k$.)

The measured spectrum is shown in Fig. 6(b), and a close agreement with the theoretical results is noticeable. Clearly, odd harmonics have larger amplitude than even harmonics, confirming the analysis of Section III-B. In fact, the first to the fifth coefficients have exactly the same value. The rest of the measured odd coefficients are more than 70 dB (3.16×10^{-4}) below the fundamental, hence, some very small deviation from the theoretical predictions (10) may be expected due to other nonmodeled effects. This deviations are also present in previous works that use more complex inverter models (see Fig. 16 in [7]).

The bound (23) is marked as a dashed line in both the figures, corresponding to a distortion level of $D = -33.9794$ dB. The dB value of the amplitude of the harmonics of the fundamental approximately decrease linearly with the frequency, and therefore, the analysis of Section III-C can be applied with $\alpha = -1$. The bound on THD computed with (26) is -33.976 dB, only slightly larger than the value of the distortion level D. On the other hand, the THD value measured with the instrument is -35.6 dB. These results confirm that the distortion level D can be used as a close approximation of the THD value, in accordance with the analysis of Section III-C.

2) Intermodulation Distortion (IMD): This test is useful to analyze the nonlinear behavior of the device under test. The PWM modulator is driven by a signal composed of the sum of a low-frequency and a high-frequency sinusoids. One of the most common standards for audio applications is SMPTE/DIN, where the high-frequency tone has 1/4 (-12 dB) of the amplitude of the low-frequency tone [25]. Typical choices for the low and high frequencies are 250 Hz and 8 kHz.

Due to the presence of the low-amplitude sinusoid, the IMD signal cannot be framed in the TEC mode, and hence, the more general expression given by (12) must be used to compute $E_p(f)$ together with (10) for the Fourier coefficients. The output current $i_o(t)$ is computed using (14). A carrier frequency of $f_c = 200$ kHz and dead-time $\Delta/T\ [\%] = 1\%$ (50 ns) were used; their amplitude are plotted in Fig. 7(a). The spectrum for zero dead-time is represented by the two components at $f_1 = 250$ Hz and $f_2 = 8$ kHz indicated by the red squares. The measured spectrum of the IMD test signal for the same modulating and carrier frequencies and dead-time values is shown in Fig. 7(b). For both cases, the amplitude of the intermodulation product at 3×250 Hz is -33.1 dB below the amplitude of the lower frequency sinusoid; the actual THD value computed with (25) is -33.72 dB and the distortion level (23), plotted in the both figures as a dashed line, results $D \approx -33.36$ dB. This limit that was slightly overestimated for the single-frequency sinusoid of the previous example, results very tight for the IMD test.

Comparison of Fig. 7(a) with Fig. 7(b) reveal that the harmonics of the lower-frequency tone and the sidebands of the

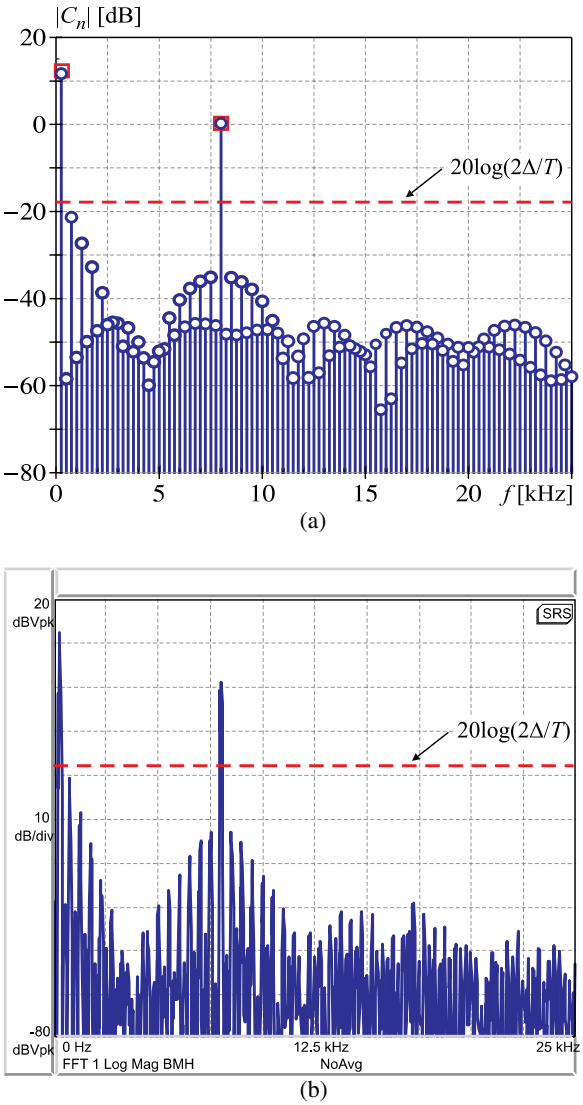

Fig. 7. PWM spectra with dead-time for an IMD test signal (250 Hz + 8 kHz), with $f_c = 200$ kHz. (a) Theoretical results and (b) measurements. (a) $\Delta = 0$ (□); $\Delta/T\ [\%] = 1\%$ (50 ns) (○). (b) $\Delta/T\ [\%] = 1\%$ (50 ns).

high-frequency component computed with (10) coincide with the measurements, and both are comprised within the bound (23). Dead-time may be thought as small deviations of the actual duty cycles to their theoretical values, and it is remarkable that variations as low as 1% of the carrier period produce a significant increase of the distortion level.

3) Line Notching: A line notching sinusoid is a standard feature of arbitrary waveform generators [20]. To analyze the influence of dead-time on a complex signal like this, a sinusoid of frequency $f_0 = 50$ Hz with six notches per period, where the second, third, fifth, and sixth pulses have half the amplitude of the first and fourth pulses, with a notch angle of $\pi/6$ and a notch width of $\pi/15$ was constructed. The signal was synthesized using 100 harmonics of its Fourier series decomposition resulting in a bandwidth of 5 kHz; the magnitude of its Fourier coefficients is shown in Fig. 8. The PWM carrier frequency is set to $f_c = 1/T = 40$ kHz.

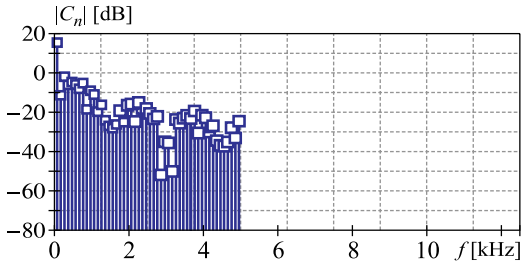

Fig. 8. Fourier series coefficients of line notching signal with zero dead-time.

As in the case of the IMD signal, the line notching signal cannot be framed in the TEC mode. The time-domain oscilloscope measurements of the filtered PWM line notch signals and the theoretical and measured spectra are depicted in Fig. 9 for $\Delta/T\ [\%] = 0.1\%$ (25 ns) and in Fig. 10 for $\Delta/T\ [\%] = 1.2\%$ (300 ns), respectively, revealing a good match between the theoretical and experimental results. The contribution of dead-time manifests as spectral leakage, with frequency components occupying a larger bandwidth than the original signal. These out-of-band harmonics (between 5 and 12.5 kHz) increase with larger dead-time values, ranging from −87.6 dB for $\Delta/T\ [\%] = 0.1\%$ to −65.5 dB for $\Delta/T\ [\%] = 1.2\%$. This experience also highlights two well-known effects of dead-time: 1) the shape of the waveforms is altered, as indicated in Fig. 10(a) because the coefficients of the fundamental and others harmonics of the signal are also modified by the dead-time; 2) the RMS voltage is reduced: a variation of 4.24% was measured for $\Delta/T\ [\%] = 1.2\%$ with respect to the RMS value corresponding to $\Delta/T\ [\%] = 0.1\%$.

The actual THD values computed with (25) gives THD [dB] = −54.97 dB for the lower dead-time and −33.53 dB for the higher dead-time, the distortion level D gives −53.98 dB and −32.39 dB, respectively. These values also confirm that D can be used as a precise estimate of the THD even for the complex signals. These distortion levels cannot be directly appreciated in the spectral measurements of Figs. 9(c) and Fig. 10(c) (as in the case of the single-frequency sinusoid or IMD signals) because the higher harmonics produced by the distortion (for example at the 3rd harmonic 150 Hz of the fundamental $f_0 = 50$ Hz) merge with the own signal harmonics. Nevertheless these distortion components are responsible for the signal degradation reflected in the temporal domain measurement of Fig. 10(a).

4) Distortion Versus Dead-Time: The relationship between D (23) and the THD [dB] was verified experimentally for three f_m/f_c ratios: $f_m/f_c = 0.02$, $f_m/f_c = 0.01$, and $f_m/f_c = 0.005$ with $\Delta/T\ [\%]$ values ranging from 0.02% to 3.5%. The THD measurements were taken with the spectrum analyzer (20 harmonics), computed as the ratio between the power with fundamental notched out and total power including fundamental. The results are summarized in Fig. 11, and are in accordance with the description in Section III-C, since D is a good approximation to the THD [dB]. It can also be observed that the bound is tighter for lower f_m/f_c ratios. This is attributed to the low-pass filtering effect of Z_L: if f_m is fixed, then with a higher f_c the attenuation of the high-frequency component of

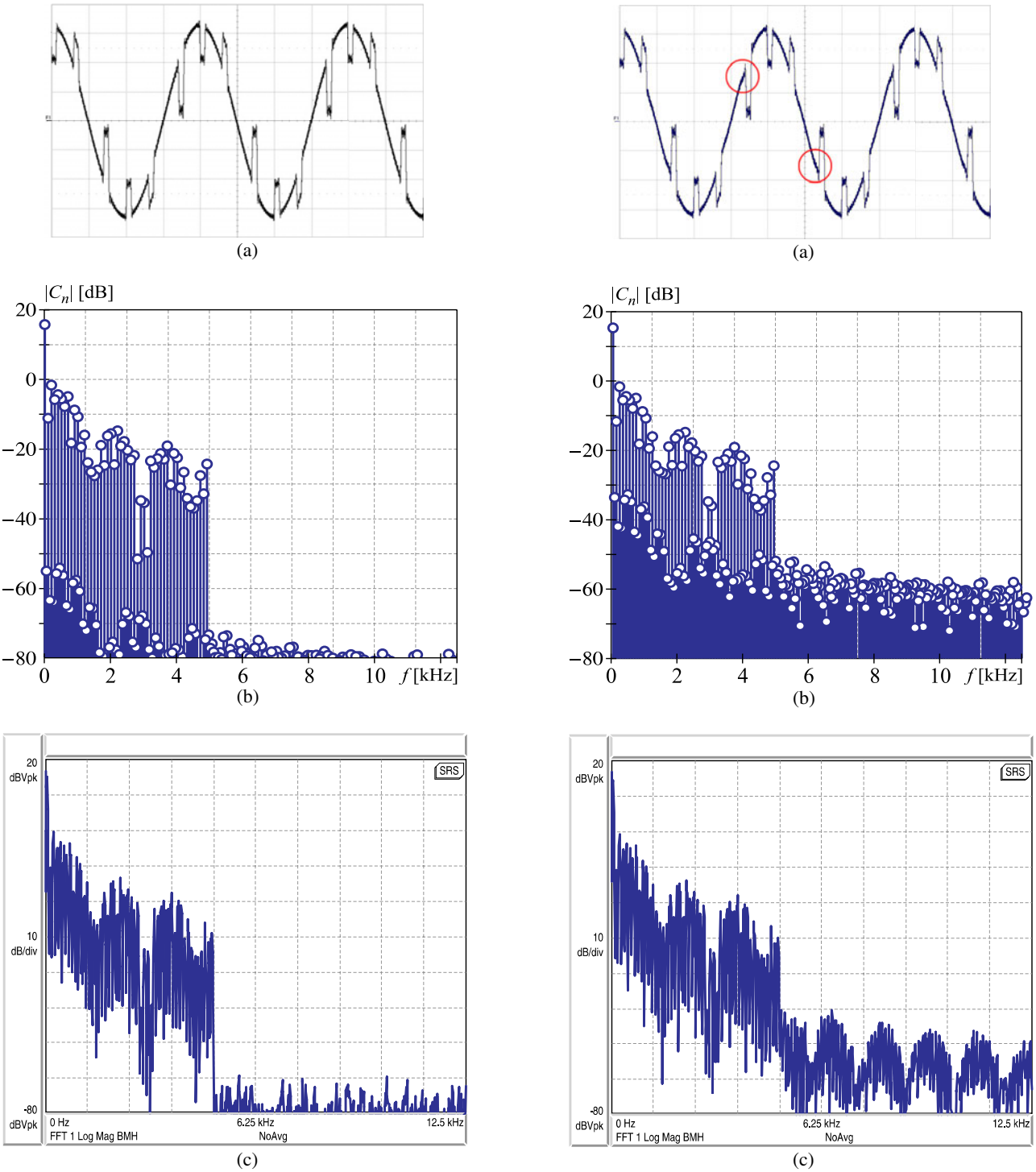

Fig. 9. Line notching; dead-time Δ/T [%] $= 0.1\%$ (25 ns); PWM frequency $f_c = 40$ kHz. (a) Time-domain waveform, (b) theoretical spectrum, and (c) measured spectrum.

Fig. 10. Line notching; dead-time Δ/T [%] $= 1.2\%$ (300 ns); PWM frequency $f_c = 40$ kHz. (a) Time-domain waveform, (b) theoretical spectrum, and (c) measured spectrum.

the current $i_{o,\mathrm{HF}}(t)$ approximated by (16) is higher, and hence, the dead-time model is even more precise.

The theoretical results do not include other sources of distortion that may be relevant for applications, such as power supply ripple rejection, inherent distortion of PWM modulators, etc. These latter effects can be reduced or ameliorated by careful design of the power stage, but dead-time effect depends on both the switching frequency and the switching speed of the power semiconductors. Due to the simplicity of calculation, D in (23) can be used as a design tool to choose these design parameters to achieve a desired distortion level. As revealed by the measurements in Fig. 11, D is a very good estimate of the THD caused by dead-time. As an example, if in a high-power application it is expected to achieve a distortion level of -40 dB from the solid

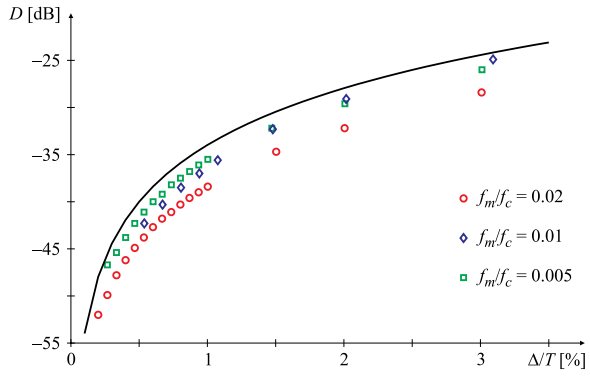

Fig. 11. Theoretical THD bound (solid line) as a function of Δ/T [%] and experimental measurements for different f_m/f_c.

line in Fig. 11 [given by (23)] results that Δ/T [%] $= 0.5\%$. If the semiconductors have a dead-time of $\Delta = 1\ \mu$s, then the maximum switching frequency must be less or equal than 5 kHz. In another application, for example in a switching audio amplifier, the expected distortion is -80 dB which results using (23) in Δ/T [%] $= 5 \times 10^{-3}\%$. If the carrier frequency is fixed at $f_c = 1/T = 100$ kHz, then switches that can operate at a dead-time of $\Delta = 0.5$ ns must be used.

V. Conclusion

The theoretical derivation of the spectrum of a PWM signal with dead-time for arbitrary band-limited modulating signals was developed. There is a close agreement between the theory and the experimental results. They also reveal that even very small dead-times highly dominate the appearance of distortion over other nonmodeled distortion sources present in the experimental setup such as switches and diodes voltage drops. The dead-time distortion analysis performed on the IMD and the line notching signals (or any other nonpure sinusoid signal) could not have been possible using previous results [4], [7], which are based on developments using the double Fourier series that is valid only for a sinusoidal modulating signal. This approach extends previous results in the literature since they are valid not only for sinusoidal type signals but also for more complex signals typically used in applications such as waveform generation and class-D amplification. Since the proposed approach is independent of the power level, the analysis can be also applied in high-power applications.

References

[1] R. Beiranvand, B. Rashidian, M. Zolghadri, and S. Alavi, "Optimizing the normalized dead-time and maximum switching frequency of a wide-adjustable-range LLC resonant converter," *IEEE Trans. Power Electron.*, vol. 26, no. 2, pp. 462–472, Feb. 2011.

[2] T. Reiter, D. Polenov, H. Probstle, and H.-G. Herzog, "PWM dead time optimization method for automotive multiphase DC/DC-converters," *IEEE Trans. Power Electron.*, vol. 25, no. 6, pp. 1604–1614, Jun. 2010.

[3] T. Itkonen, J. Luukko, A. Sankala, T. Laakkonen, and R. Pollanen, "Modeling and analysis of the dead-time effects in parallel PWM two-level three-phase voltage-source inverters," *IEEE Trans. Power Electron.*, vol. 24, no. 11, pp. 2446–2455, Nov. 2009.

[4] C. Wu, W.-H. Lau, and H. S.-H. Chung, "Analytical technique for calculating the output harmonics of an H-bridge inverter with dead time," *IEEE Trans. Circuits Syst. I, Fundam. Theory Appl.*, vol. 46, no. 5, pp. 617–627, May 1999.

[5] W. Lau, B. Zhou, and H. Chung, "Compact analytical solutions for determining the spectral characteristics of multicarrier-based multilevel PWM," *IEEE Trans. Circuits Syst. I, Reg. Papers*, vol. 51, no. 8, pp. 1577–1585, Aug. 2004.

[6] F. Koeslag, H. Mouton, and H. Beukes, "An investigation into the separate and combined effect of pulse timing errors on harmonic distortion in a class D audio amplifier," in *Proc. IEEE Power Electron. Spec. Conf.*, 2008, pp. 1055–1061.

[7] F. Koeslag, H. D. Mouton, and J. Beukes, "Analytical modeling of the effect of nonlinear switching transition curves on harmonic distortion in class D audio amplifiers," *IEEE Trans. Power Electron.*, vol. 28, no. 1, pp. 380–389, Jan. 2013.

[8] H. B. Black, *Modulation Theory*. Princeton, NJ, USA: Van Nostrand, 1953.

[9] D. C. Moore, M. Odavic, and S. M. Cox, "Dead-time effects on the voltage spectrum of a PWM inverter," *IMA J. Appl. Math.*, pp. 1–16, Feb. 2013. Available: http://imamat.oxfordjournals.org/content/early/2013/02/05/imamat.hxt006.abstract

[10] Z. Song and D. Sarwate, "The frequency spectrum of pulse width modulated signals," *Signal Proc.*, vol. 83, no. 10, pp. 2227–2258, 2003.

[11] F. Chierchie and E. Paolini, "Quasi-analytical spectrum of PWM signals with dead-time for multiple sinusoidal input," in *Proc. IEEE Int. Symp. Circuits Syst.*, May 2011, pp. 1033–1036.

[12] I. Mosely, P. Mellor, and C. Bingham, "Effect of dead time on harmonic distortion in class-D audio power amplifiers," *Electron. Lett.*, vol. 35, no. 12, pp. 950–952, Jun. 1999.

[13] K. S. Low, "A DSP-based single-phase ac power source," *IEEE Trans. Ind. Electron.*, vol. 46, no. 5, pp. 936–941, Oct. 1999.

[14] Y. Jun, T. T. Meng, S. Cox, and G. Wang-Ling, "Time-domain analysis of intermodulation distortion of closed-loop class-D amplifiers," *IEEE Trans. Power Electron.*, vol. 27, no. 5, pp. 2453–2461, May 2012.

[15] K. L. Chun, T. T. Meng, S. Cox, and S. Y. Kiat, "Class-D amplifier power stage with PWM feedback loop," *IEEE Trans. Power Electron.*, vol. 28, no. 8, pp. 3870–3881, Aug. 2013.

[16] O. Senturk and A. Hava, "Performance enhancement of the single-phase series active filter by employing the load voltage waveform reconstruction and line current sampling delay reduction methods," *IEEE Trans. Power Electron.*, vol. 26, no. 8, pp. 2210–2220, Aug. 2011.

[17] M. Herran, J. Fischer, S. Gonzalez, M. Judewicz, and D. Carrica, "Adaptive dead-time compensation for grid-connected PWM inverters of single-stage PV systems," *IEEE Trans. Power Electron.*, vol. 28, no. 6, pp. 2816–2825, Jun. 2013.

[18] X. Zha and Y. Chen, "The analysis and compensation of dead-time effects on active power filter in α-β coordinate," in *Proc. Int. Conf. Elect. Mach. Syst.*, 2008, pp. 2045–2048.

[19] Y. Zhang and J. Zhu, "A novel duty cycle control strategy to reduce both torque and flux ripples for DTC of permanent magnet synchronous motor drives with switching frequency reduction," *IEEE Trans. Power Electron.*, vol. 26, no. 10, pp. 3055–3067, Oct. 2011.

[20] N. Mohan, T. M. Undeland, and W. P. Robbins, *Power Electronics: Converters, Applications, and Design*. New York, NY, USA: Wiley, 2002.

[21] H. Mouton and B. Putzeys, "Understanding the PWM nonlinearity: Single-sided modulation," *IEEE Trans. Power Electron.*, vol. 27, no. 4, pp. 2116–2128, Apr. 2012.

[22] A. Oppenheim, R. Schafer, and J. Buck, *Discrete-Time Signal Processing*. Englewood Cliffs, NJ, USA: Prentice-Hall, 1989.

[23] D. G. Holmes and T. A. Lipo, *Pulse Width Modulation for Power Converters: Principles and Practice*. New York, NY, USA: Wiley-IEEE Press, 2003.

[24] L. Stefanazzi, A. Oliva, and E. Paolini, "Alias-free digital click modulator," *IEEE Trans. Ind. Informat.*, vol. 9, no. 2, pp. 1074–1083, May 2013.

[25] B. Metzler, *Audio Measurement Handbook*. Beaverton, OR, USA: Audio Precision, 1993.

Fernando Chierchie (GS'10) received the B.S. degree in electronic engineering and the M.S. degree in control systems both from Universidad Nacional del Sur, Bahía Blanca, Argentina, in 2009 and 2011, respectively.

He is currently a Ph.D. student and Teaching Assistant of Digital Signal Processing at the Universidad Nacional del Sur. His research interests include switching amplifiers, signal processing, power electronics, and DSP implementations of digital control and signal processing algorithms.

Leandro Stefanazzi received the B.S. degree in electronic engineering, the M.S. in control systems and the Ph.D. degree from Universidad Nacional del Sur, Bahía Blanca, Argentina in 2006, 2008, and 2013, respectively.

From June 2009 to November 2010, he joined the Electronics and Information Technology Laboratory of the French Atomic Energy Commission (CEA-LETI) as a Research Engineer in the areas of communications for 3GPP/LTE standards. His research interests include digital signal processing and power electronics.

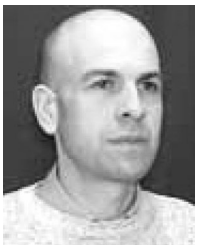

Eduardo E. Paolini received the B.S. degree in electrical engineering from the Universidad Nacional del Sur, Bahía Blanca, Argentina, in 1987.

He is an Adjunct Professor at Universidad Nacional del Sur, Bahía Blanca, Argentina, since 1998, and a member of Comisión de Investigaciones Científicas de la Provincia de Buenos Aires since 2011. His research interests include digital signal processing, and switched and nonlinear systems.

Alejandro R. Oliva received the B.S. degree in electrical engineering from the Universidad Nacional del Sur in 1987, and the Master's and Ph.D. degrees in electrical engineering from the University of Arkansas, Fayetteville, AR, USA, in 1996 and 2004, respectively.

He is currently a Professor at the Department of Electrical Engineering, Universidad Nacional del Sur, Bahía Blanca, Argentina, since 1999. Since 2005, he is a member of CONICET. His main research interests include power electronics and power management.